Indian Journal of Biochemistry & Biophysics
Vol. 62, September 2025, pp. 998-1006
DOI: 10.56042/ijbb.v62i9.16613

Exploration of DNA binding mode of Coumarin Glycoside Esculin by Multispectral and Molecular dynamics approaches

Poonam R Inamdar[1]*, Vishnu P Chaudhari[1], Shashikant V Bhandari[2], Somdatta Chaudhari[3] & Pranali Polshettiwar[1]

[1]Department of Pharmaceutical Sciences, School of Health Sciences and Technology, Dr Vishwanath Karad MIT World Peace University, Pune-411 038, Maharashtra, India

[2]Department of Pharmaceutical Chemistry, AISSMS College of Pharmacy, Kennedy Road, Pune-411 001, Maharashtra, India

[3]PES Modern College of Pharmacy, Nigdi, Pune-411 044, Maharashtra, India

Received 23 January 2025; *revised 22 March 2025*

Due to the unwanted and undesired effects of existing anticancer agents, medicinal chemists are exploring drugs from natural origin. Phytochemicals and their derivatives can be developed as Biologically diverse agents with fewer side effects. Therefore, exploration of the different biological activities of natural products had been a keen interest in repurposing of the drugs. Present study focuses on the analysis of DNA (Deoxyribonucleic Acid) interactions of esculin using spectroscopic and molecular docking, simulation techniques, and MMGBSA (Molecular Mechanics Generalizing Born Surface Area) calculations. We used different spectral techniques to investigate the interactions of esculin with DNA. FTIR (Fourier Transform Infra Red Spectroscopy) spectral studies suggested the primary formation of non-covalent bond between esculin and the nitrogen base of DNA, stating the primary analysis of interactions. The observation revealed that the UV-visible (UltraViolet) spectra of esculin exhibited perturbations in the presence of CT (Calf thymus) DNA and interacted with DNA in the groove binding mode. The hyperchromic effect was determined by the increase in the absorbance value of esculin in the presence of DNA, and the binding constant (K_b) value of esculin was $2.327 \pm 0.09 \times 10^3$ M^{-1}. By conducting circular dichroism and viscometric analysis of DNA in the presence of esculin, we could support the groove binding mode of esculin. In Silico studies suggested that esculin has bound in the major groove between the base pairs with 6 Hydrogen bond interactions with different nucleobases. Molecular simulation analysis supported the results with lowest RMSD (Root mean square deviation), stating the stable complex of PDB (Protein Data Base) and esculin. MMGBSA analysis suggested that significant contributions from van der Waals interactions made the overall binding favorable. These findings can lead to design of DNA interacting esculin based derivatives exhibiting the anticancer potential.

Keywords: DNA interaction studies, Esculin, Groove binding mode, MMGBSA calculations, Spectroscopic studies

Natural products are contributing to the new advances in therapeutics. They are chemically stable, compatible. Natural products exhibit less toxicity and side effects. Coumarins are the widely explored natural compounds. Coumarins possess diverse beneficial characteristics.

Coumarins are chemically known as benzo-α-pyrones. They are polyphenols reported for a versatile range of biological activities[1-3]. Esculin, (6-beta-glucoside-7-hydroxycoumarin, molecular formula: $C_{15}H_{16}O_9$) is a glycosidic coumarin derivative. The 2 parts of the molecule (glucose and 7-hydroxycoumarin) are linked by an ester linkage through oxygen. The authentic Chinese traditional medicine *Cortex Fraxini* is considered the source for esculin[4-6]. It has exhibited anti-inflammatory, antitumor, antibacterial, antifungal, and antithrombotic activities [7,8.]

Despite of reports of various biological activities, esculin is not yet explored for its DNA binding ability. Thus, it is significant to understand the mode of binding of esculin with DNA It may lead to the development of derivatives of esculin possessing anticancer potential.

Interaction of small organic molecules with biological macromolecules such as DNA has been a topic of great interest. DNA interacting agents can be developed into potent therapeutic agents. DNA is considered the prime target for the development of various pharmacological agents such as anticancer, antimicrobial, and antiviral agents. Exploration of DNA binding ability of the drugs is significant.DNA binding agents bind to the DNA through non-covalent, hydrogen bond and van der waals interactions which may control DNA replication and

---

*Correspondence:
E-mail: poonam.inamdar@mitwpu.edu.in
Suppl. data available on respective page of NOPR

gene expression [9.] Base pair arrangement, hydrogen-accepting groups as OH and PO_4— functional groups, conformational stabilityand predictable structural changes post binding makes DNA a perfect target compared to drug-targeting proteins for the development of therapeutic agents. Therefore, there is an increase in the research of the development of novel effective medications that target DNA. Thus, advanced research needs to recognize the binding mechanism and the binding affinities between bioactive molecules and DNA.

In the present study, we investigated the DNA binding ability of Esculin. Primary analysis of interaction was carried out by Fourier Transform Infrared (FTIR) spectroscopy. Later, we utilized the UV visible spectrophotometric titration to ascertain the mode of binding of esculin with DNA. To correlate the predicted binding mode of esculin, circular dichroism, and viscometric studies were carried out. Furthermore, In silico molecular docking techniques enabled us to find the mode of interaction of esculin with specific nucleobases in the DNA groove. Molecular dynamic studies postulated the structural stability of the complex of esculin and DNA. MMGBSA analysis performed also suggested that overall binding seems favourable by significant contributions from interactions. As esculin, is a natural plant-derived bioactive compound, analysing its interactions with biomolecules may guide to the development of effective therapeutic agents.

Experimental Section

Materials

Calf thymus DNA was procured from Sigma Aldrich. The purity of the procured CT DNA was checked at wavelengths of 260 nM and 280 nM using UV spectroscopy. Tris HCl was used as a buffer for DNA binding experiments and was purchased from sigma Aldrich. Esculin, was procured from Yucca enterprise, Mumbai. The purity of theprocured esculin was 98%.

Instrumentation

DNA binding UV experiments were performed on Shimadzu 1900 I instrument spectrophotometer.FTIR analysis of the esculin and DNA was carried out on Shimadzu IR QATRS model. Conformational analysis of DNA after binding of esculin was carried out using Circular Dichroism technique on instrument JASCO J-7 spectropolarimeter.

Preparation of solutions

0.1M Tris HCl buffer was prepared using distilled water. The pH of buffer was maintained at pH 7.2. The purity of CT DNA was checked using UV spectroscopy and the absorption ratio of procured calf thymus DNA in a buffer was checked and the absorption ratio (A_{260}/A_{280}) was found to be 1.9:1, giving an idea of protein free DNA. The concentration of DNA was determined using molar extinction coefficient of $6600M^{-1}cm^{-1}$ at λ_{max} 260 nM.

Methods

Fourier transform infrared (FTIR) spectroscopic method

FTIR spectra were measured on a Shimadzu IR QATRS model. FTIR spectrum of blank DNA, blank esculin and esculin + DNA was recorded and compared for the analysis of primary level binding of esculin with DNA. Esculin and DNA mixture was incubated for 2h and then subjected for the FTIR analysis.

Electronic absorption spectroscopic method

A stock solution of esculin (10mM) was prepared by dissolving in 1:10 as water: buffer at pH 7.2. DNA binding studies of esculin were performed using solution of esculin of concentration 30 μM. UV spectrum of esculin is monitored after the successive additions of CT DNA (0 -240 μM). Base line correction was carried out using blank solution containing of CT-DNA in Tris-HCl buffer.

Circular dichroism method

Circular dichroism analysis was carried out using spectropolarimeter. Analysis was done separately for CT DNA (100 μM) alone as first sample and CT DNA in the presence ofesculin as second sample. The changes in the conformations were compared before and after binding of the esculin.

Viscosity measurements

For viscosity measurements, the ubbelohde viscometer (1mL capacity) was used and the efflux time for each sample was measured and the flow time was calculated. The rate of flow for the buffer (10mM Tris), DNA (100 μM) and DNA in the presence of varying concentrations (0 - 150 μM) of esculin were measured and the relative specific viscosity (η) was calculated.

Molecular docking studies

Molecular docking study was carried out using an Autodock vina[10, 11](http://vina.scripps.edu/) and MGL tools[12] (http://mgltools.scripps.edu/) of The Scripps research Institute. DNA (pdb ID: 1BNA)was modified by adding polar hydrogens and removing water molecules. The grid points of 30 × 26 × 34with 1.0 Å spacing were calculated around the docking area for all the ligand atom types using default optimization parameters. Esculin was saved in pdbqt format by keeping it's torsional bonds intact. A PyMOL[13] molecular viewer was used to analyze the docking results and images. Lowest energy conformer of esculin was selected for the best docking pose.

Molecular dynamic studies

Molecular dynamics study was carried out using Desmond 2020.1from Schrödinger, LLC. The OPLS-2005 force field[14-16]and explicit solvent model with the TIP3P water molecules were used in this system[17].The boundary salvation box of 10 Å x 10 Å x 10 Å dimensions. Na^+ ions were added to neutralize the charge 0.15 M, and NaCl solutions were added to the system to simulate the physiological environment. Initially, the system was equilibrated using an NVT ensemble for 10 ns to retrain over the protein-ligand complexes. Following the previous step, a short run of equilibration and minimization was carried out using an NPT ensemble for 12 ns. The NPT ensemble was set up using the Nose-Hoover chain coupling scheme[18]with varying temperatures, relaxation time of 1.0 ps, and pressure of 1 bar in all the simulations. A time step of 2fs was used. The Martyna-Tuckerman–Klein chain coupling scheme[19]barostat method was used for pressure control with a relaxation time of 2 ps. The particle mesh Ewald method[20]was used for calculating long-range electrostatic interactions, and the radius for the coulomb interactions was fixed at 9Å. The final production run was carried out for 100 ns. The root means square deviation (RMSD), the radius of gyration (Rg), root mean square fluctuation (RMSF), and a number of hydrogen (H-bonds), are calculated to monitor the stability of the MD simulations.

Binding free energy analysis

The molecular mechanics combined with the generalized Born surface area (MM-GBSA) approach was used to compute the binding free energies of the ligand-protein complexes. The Prime MM-GBSA binding free energy was calculated using the Python script thermal mmgbsa.py in the simulation trajectory for last 50 frames with a 1-step sampling size. The binding free energy of Prime MM-GBSA (kcal/mol) was estimated using the principle of additivity, in which individual energy modules such as columbic, covalent, hydrogen bond, van der Waals, self-contact, lipophilic, solvation of protein and ligand were collectively added. The equation used to calculate ΔG_{bind} is the following:

$$\Delta G_{bind} = \Delta G_{MM} + \Delta G_{Solv} - \Delta G_{SA}$$

Whereas;

ΔG_{bind} designates the binding free energy, ΔG_{MM} designates the difference between the free energies of ligand-protein complexes and the total energies of protein and ligand in isolated form, ΔG_{Solv} designates the difference in the GSA solvation energies of the ligand-receptor complex and the sum of the solvation energies of the receptor and the ligand in the unbound state, ΔG_{SA} designates the difference in the surface area energies for the protein and the ligand.

Results and Discussion

FTIR spectroscopic analysis

FTIR is a technique based on the change in the length and angles of the bonds of compounds after the absorption of IR waves. We investigated primary interaction between esculin and CT DNA using FTIR analysis. FTIR spectrum confirms the presence of guanine base at 1713 cm^{-1}, exhibiting intense peak[21]as depicted in (Suppl. Fig. 1). A broader peak at 3600 cm^{-1} confirms the presence of free hydroxyl groups present in the glucoside part of the esculin. In the Suppl. Figure 2, the FTIR spectrum of esculin has exhibited a sharp and intense peak at 1720 cm^{-1} showing the presence of carboxyl functionality in the structure of esculin. Post incubation, FTIR spectrum of esculin + DNA, depicted in (Fig. 1), shows the presence of phosphate group at 1200 cm^{-1} with an intense peak which might be because of helix destabilization post interaction. It was also noted that the intensity of transmittance of Guanine base at 1713 cm^{-1} was quenched in the presence of esculin. This supports the primary interaction between esculin and DNA.

Electronic absorption spectroscopic analysis

Mode of binding of esculin to CT DNA was determined using UV absorption titration. The UV spectrum of 30 μM solution of esculin in the absence of CT DNA and with successive increment of CT DNA is shown in (Fig. 2). The absorption maxima of esculin observed in the range of 335 nM – 339 nM.

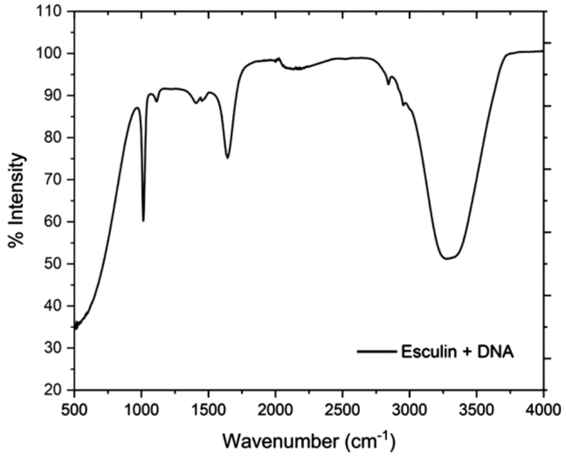

Fig. 1 — FTIR Spectrum of Esculin and DNA

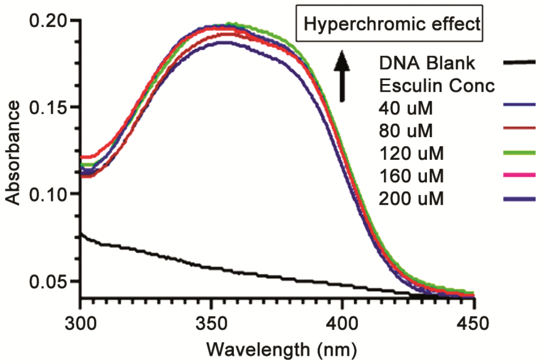

Fig. 2 — UV absorption titration spectrum of esculin in the presence of increments of DNA

The λ_{max} of the esculin was focused for the changes in the absorbance value and shifts in the wavelength post addition of DNA. UV spectrum of esculin exhibited hyperchromic effect with increasing amounts of DNA. Hyperchromism can be characterized by increase in the absorbance value without the shift in the value of absorption maxima. The hyperchromic effect states the groove binding mode of the esculin[22,23]. Major and minor grooves of DNA possess potential H bonding regions along with nucleotides having hydrogen bond donors as well as hydrogen bond acceptors[24-26].

Esculin has a free –OH group on the coumarin ring, contributing as hydrogen atom donor group. It may take part in formation hydrogen bond interactions in the groove of DNA. An attached glucoside moiety may also have played an important role in the groove binding of the esculin due to the presence of planar free –OH groups.

Intrinsic binding constant $K_b$value of esculin was calculated on the basis of readings obtained from absorption spectral titration using formula[23]:

$$[DNA] / (\varepsilon_a - \varepsilon_f) = [DNA] / (\varepsilon_a - \varepsilon_f) + 1/ K_b (\varepsilon_b - \varepsilon_f) \ldots (1)$$

where, $\varepsilon_{a,}$ ε_f and ε_b correspond to A_{obsd}/[esculin/DNA], the extinction coefficients for free esculin/DNA and that of esculin/DNA in fully bound form, respectively. [DNA] / (ε_a- ε_f) vs [DNA] values were plotted and $K_b$was obtained as the ratio of the slope to the intercept. Intrinsic binding constant for esculin was found to be $(2.33\pm\ 0.16)\times 10^3 M^{-1}$respectively.Apparently, esculin has a high K_b value, proving to possess satisfactory binding affinity. Presence of glucosidic ring changes the conformation of the esculin causing it to adjust between the base pairs of groove of DNA.

Gibbs free energy change (ΔG) of esculin was calculated using K_b, binding constant value. ΔG gives an idea of spontaneity / non-spontaneity of esculin-DNA and. ΔG was calculated using K_b, binding constant value of esculin as;

$$\Delta G = -2.303\ RT\ (\log_{10} K_b)\ [KJ/mol] \qquad \ldots (2)$$

A free energy change for esculin was found to be -16.62KJ/mol favoring the spontaneous binding ability of esculin with DNA.

Circular dichroism studies analysis

Conformation is the characteristic quality of DNA helix. Intercalating agents change the conformation of DNA after binding. These changes in the conformational properties of DNA aremonitored by Circular dichroism spectroscopy[27-29]. Binding mode of esculin was confirmed on the basis of change in the conformation of DNA. Plain DNA and esculin along with DNA were assessed for the change in the conformation. It is reported that the typical right handedB-DNA exhibits the peak at 277 nM. It is due to the base stacking property of DNA. Another peak observed at 246 nM due to helical nature of DNA[30,31]. Generally, intercalator stacks axially between the base pairs of DNA causing increase in the chain length of DNA. An increased chain length of DNA affects the helical pattern of DNA.On the other hand, agents who bind in the groove of DNAdoes not cause any shifts in the intensities of positive and negative bands of DNA, as they do not cause change in the length of DNA[32,33].

In the presence of increased concentration of the esculin, the decrease in the positive band along with the remarkable blue shift of 2-3 nM respective to the position of the standard DNA band was observed in the (Fig. 3). It can be postulated that the groove binding mode of esculin has not affected conformation and helicity of the DNA significantly[34].

Thus, esculin clearly rules out the standard intercalative mode of binding.

Viscosity measurement analysis

As hydrodynamic parameters are sensitive tochanges post interaction, binding of esculin in the groove may have affected the chain length in a different manner[35]. In order to understand in detail, viscosity studies were carried out with solutions of DNA incubated along with esculin. A comparison of the flow rates of buffer, the DNA (100 μM) and the DNA incubated with esculin at various concentrations (25 -200 μM) were monitored. The relative specific viscosity was calculated, using equation $(t - t_0)/ t_0$, where t_0 stands for the flow time of buffer and t for flow time for DNA in the presence and absence of the esculin. Plot of $(\eta/\eta_0)^{1/3}$vs 1/R (R = [esculin]/[DNA]) is presented in (Fig. 4), where η is the viscosity of DNA in the presence of varying concentrations of esculin and η_0 is the viscosity of the DNA alone. With increasing concentrations of esculin in DNA, caused only minimal changes in the viscosity supporting their DNA groove binding nature.

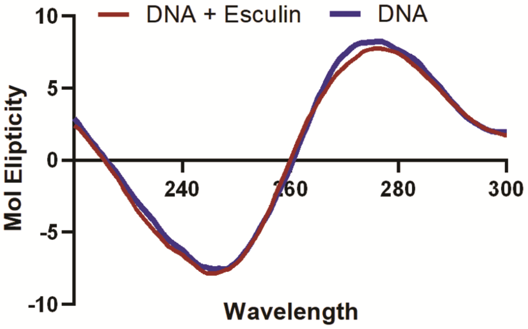

Fig. 3 — Circular Dichroism spectrum of DNA and DNA+Esculin

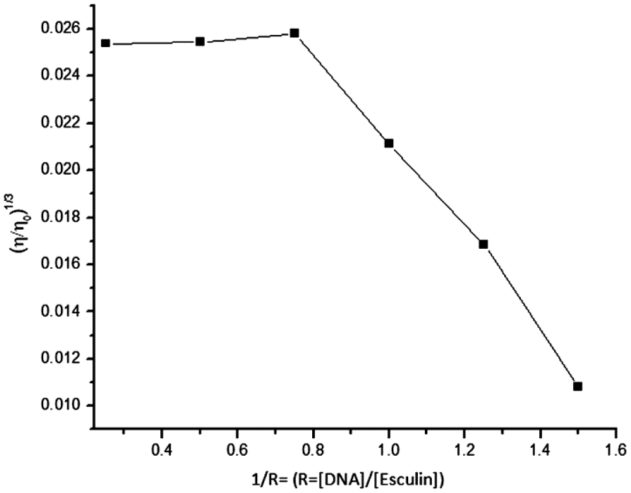

Fig. 4 — Relative viscosity $(\eta/\eta_0)^{1/3}$of the DNA in the presence of increments of Concentration of Esculin

Molecular docking studies

To get a detailed perception of the binding behaviour of the complexes, a docking study was carried out using a selected DNA sequence (PDB ID: 1BNA). According to the results obtained, esculin was found to interact with the DNA through a groove. Figure 5 shows the docking image of esculin with PDB 1BNA.

Best possible conformer of esculin was generated from Autodock Vina and studied thoroughly for the docking. It has been noted that esculinis stabilized at DNA major groove through six hydrogen bond interactions as shown in (Fig. 6) with binding energy -7.81 kcal/mol (Table 1). Hydroxyl groups of glucoside part of the esculin have participated in the H bond interactions. Hydrogen atom of first OH group of glucosidicpart of the esculin creates H bond with the oxygen of phosphate group attached to deoxyadenine 5 (DA 5) at a distance of 1.7 A.U. Hydrogen atom of second OH group of glucosidicpart of the esculin creates H bond with the oxygen of carbonyl group attached to deoxyadenine 5 (DA 5) at a distance of 2.5 A.U. Hydrogen atom of third OH

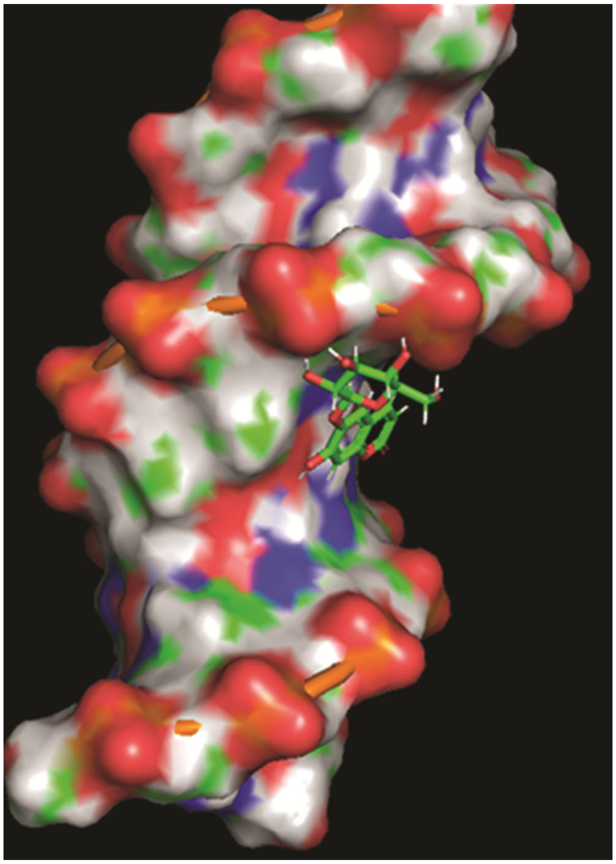

Fig. 5 — Esculin binding in the major groove of DNA (PDB ID: 1BNA)

group of glucosidic part of the esculin creates H bond with the oxygen of phosphate group attached to deoxyadenine 6 (DA 6) at a distance of 2.7 A.U. Hydrogen atom of fourth OH group of glucosidic part of the esculin creates H bond with the oxygen of phosphate group attached to deoxyadenine 6 (DA 6) at a distance of 2.8 A.U. Hydrogen atom of OH group present on coumarin ring creates H bond with carbonyl group of acidic functionality of Deoxythymidine 7 (DT7) at a distance of 2.7 A.U. Oxygen atom present in the coumarin ring creates H bond with hydrogen atom of hydroxyl group of amino group of deoxyadenine 16 (DA 16) at a distance of 2.2 A.U.Thus, molecular docking throws light on the binding nature of esculin to DNA proving through its covalent and H bond interactions[36,37].

Molecular Dynamic Simulation Studies

Molecular dynamics and simulation (MD) studies were carried out to determine the stability and convergence of 1BNA_Esculin. The Figure 7A illustrates the Root Mean Square Deviation (RMSD) values of the 1BNA_Esculin complex over a simulation period of 100 nanoseconds (ns). RMSD is a common measure used to evaluate the stability and conformational changes of a molecular system over time. The RMSD values start around 2 Å and fluctuate between 2 Å and 3 Å. This indicates initial adjustments of the system as it equilibrates. During this period, the RMSD continues to fluctuate, showing

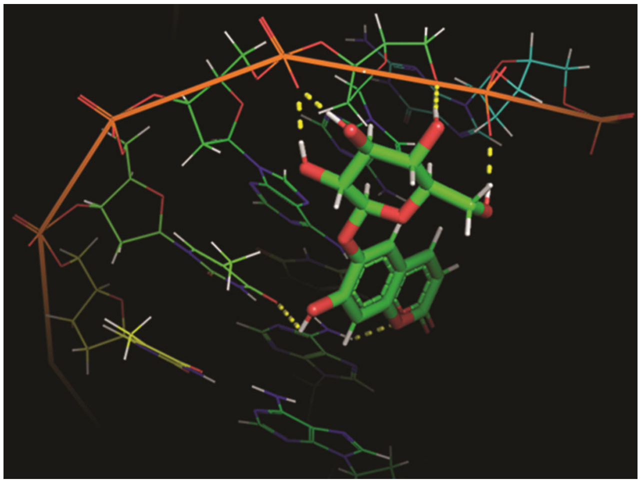

Fig. 6 — Hydrogen bond interactions ofEsculin in the major groove of DNA (PDB ID: 1BNA)

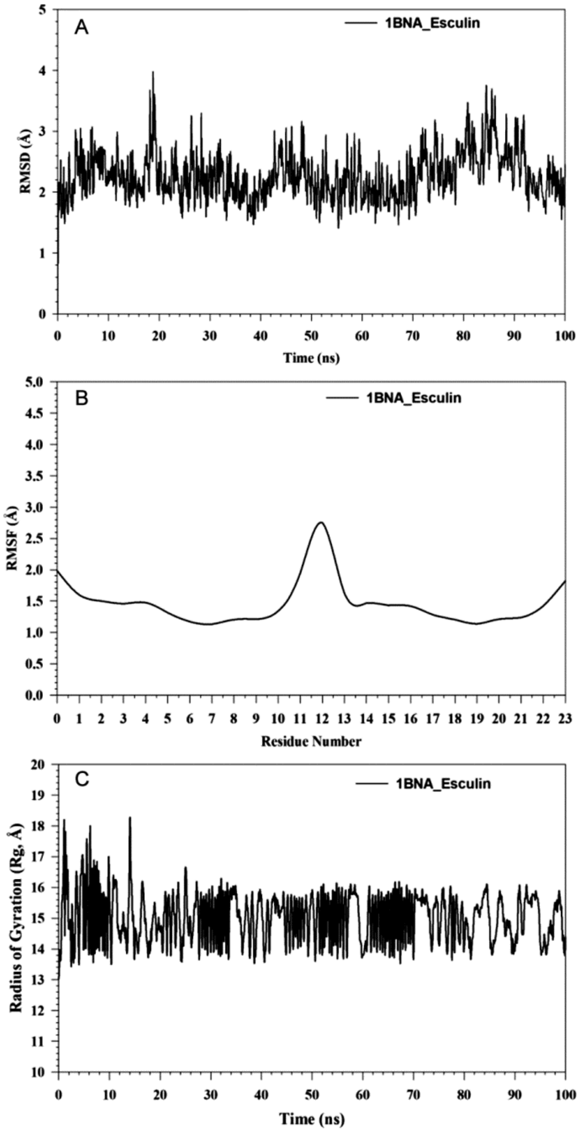

Fig. 7 — MD simulation analysis of 100 ns trajectories of (A) RMSD of Cα backbone of 1BNA_Esculin(B) RMSF of Cα backbone of 1BNA_Esculin (C) Radius of gyration (Rg) of Cα backbone of1BNA_Esculin

Table 1 — Molecular docking Parameters of Esculin

Compound	Binding Energy (kcal/mol)	Number of Hydrogen Interactions		
Esculin	-7.8	6		
		Name and No of Nucleobase	Atom of Str of Esculin	Distance of Interaction (AU)
		O of PO_4^- of DA5	O of OH of glucoside Unit	1.7
		O of CO of DA5	H of OH of glucoside Unit	2.5
		O of PO_4^- of DA6	O of OH of glucoside Unit	2.7
		O of PO_4^- of DA6	O of OH of glucoside Unit	2.8
		H of NH of DA16	O of Coumarin Ring	2.7
		O of C=O of DT7	O of OH of coumarin	2.2

transient increases up to 3 Å but predominantly stays within the 2-3 Å range. This suggests that the system maintains a relatively stable conformation with minor deviations. There is a noticeable increase in fluctuations, with RMSD values occasionally spiking above 3 Å and approaching 4 Å. This indicates larger conformational changes in the system towards the end of the simulation. Despite the fluctuations, the Average RMSD value was around 2.27 Å for most of the simulation suggest that the 1BNA_Esculin complex is relatively stable. Significant deviations beyond 3 Å, particularly towards the end, might indicate regions of the protein or ligand that are more flexible or undergoing conformational transitions. The Figure 7B depicts the Root Mean Square Fluctuation (RMSF) values of the residues in the 1BNA_Esculin complex. RMSF is used to analyze the flexibility of individual residues in a molecular dynamic's simulation. RMSF values range from approximately 1.13 Å to 2.75 Å, with a significant peak reaching close to 4 Å around residue number 12. The majority of the residues exhibit RMSF values between 1.0 Å and 2.0 Å, indicating that these regions are relatively stable. The notable peak around residue number 12 suggests increased flexibility or motion in this part of the complex. The RMSF analysis highlights the dynamic behavior of the 1BNA_Esculin complex at the residue level. Most residues exhibit low RMSF values, indicating stability, while the significant peak at residue 12 suggests a functionally important flexible region. The Figure 7C illustrates the Radius of Gyration (Rg) values of the 1BNA_Esculin complex over a simulation period of 100 nanoseconds (ns). Rg measures the distribution of atoms around the centre of mass of a molecule and is an indicator of the compactness and overall structural changes of the complex during the simulation. The Rg values start around 13.03 Å and show considerable fluctuation, reaching up to 18.08 Å. During this period, the Rg values fluctuate between 13 Å and 16 Å, with occasional peaks. The fluctuations are more frequent but within a relatively stable range. The Rg values show a pattern similar to the mid-simulation phase, with values predominantly between 13 Å and 16 Å and occasional peaks. The Rg analysis indicates that the 1BNA_Esculin complex maintains a relatively stable and compact structure throughout the 100 ns simulation. The initial phase shows significant structural adjustments, followed by a stable period with minor fluctuations. Occasional expansions are also observed in the $R_g$values suggesting dynamic behavior without compromising overall structural integrity.

Molecular Mechanics Generalized Born Surface Area (MM-GBSA) calculations

Utilizing the MD simulation trajectory, the binding free energy along with other contributing energy in form of MM-GBSA were determined for 1BNA_Esculin. The results (Table 2) suggested that the binding energies (ΔG_{bind}) for the 1BNA_Esculin complex is -12.31 ± 2.14 kcal/mol. This negative value indicates thatbinding process is energetically favorable and spontaneous under standard conditions. The relatively low standard deviation suggests consistency in the binding affinity measurements. The Coulombic energy contribution is 213.20 ± 22.54 kcal/mol. This large positive value reflects the electrostatic interactions between the binding partners. Although the electrostatic interactions are strong, they alone are not sufficient to drive the binding process towards being favorable. The covalent energy contribution is 1.18 ± 0.74 kcal/mol. This relatively small value indicates minor changes in the covalent bonding network upon binding, suggesting that covalent interactions are not a significant driving force in the binding of 1BNA to Esculin. The lipophilic contribution to the binding free energy is -2.68 ± 0.41 kcal/mol. The negative value here indicates that hydrophobic interactions favor binding, as lipophilic interactions typically stabilize the complex by reducing the unfavorable entropy associated with solvent-exposed hydrophobic regions. The solvation energy contribution is -201.92 ± 21.29 kcal/mol. This significant negative value suggests a strong solvation effect, likely due to favorable desolvation of polar or charged groups upon binding. This term helps to balance the large positive Coulombic energy, contributing to the overall favorable binding free energy. The van der Waals energy contribution is -22.08 ± 1.38 kcal/mol. This negative value indicates that van der Waals forces are a significant stabilizing factors in the binding process. It is highlighting the importance of favorable dispersion interactions between 1BNA and Esculin. The binding of 1BNA to Esculin is

Table 2 — Binding free energy components for the 1BNA_Esculin calculated by MM-GBSA

Energies (kcal/mol)	1BNA_Esculin
ΔG_{bind}	-12.31±2.14
ΔG_{bind}Coulomb	213.20±22.54
ΔG_{bind}Covalent	1.18±0.74
ΔG_{bind}Lipo	-2.68±0.41
ΔG_{bind}SolvGB	-201.92±21.29
ΔG_{bind}VdW	-22.08±1.38

driven by a combination of various interaction forces. Despite the large positive value of Coulombic energy, the overall binding is made favorable by significant contributions from van der Waals interactions, lipophilic interactions, and especially the solvation effects. The balance between these forces results in a net negative binding free energy, indicating a spontaneous and energetically favorable interaction.

Conclusion

The mode of binding of the coumarin glycoside esculin to CT DNA was explored using spectroscopic and In Silico Techniques. FTIR spectral studies were used to conduct primary interaction studies between CT DNA and esculin. According to the FTIR Spectral analysis, the esculin was bonding to guanine base of DNA through, weak hydrogen bonds. Furthermore, DNA binding mode of the esculin was ascertained by UV visible spectral titrations. It exhibited hyperchromism at the λ_{max} of the esculin, *i.e.* 337 nM. The increase in the absorbance of esculin without a red shift indicates the hyperchromic effect and thus, the results, concluded the groove binding mode. The binding constant (K_b) valuefor esculin was found to be (2.33± 0.16) × $10^3 M^{-1}$. Later, circular dichroism studies were performed to analyse the conformational changes in the DNA in the presence of esculin. It postulated that esculin clearly ruled out the standard intercalative mode of binding, as the change in the 3D conformation of the DNA was negligible due to the groove binding mode of esculin. Viscosity measurement studies also supported the groove binding mode of esculin. Furthermore, *in silico*, molecular docking studies were carried out to support the binding efficacy of esculin to DNA. Esculin interacted DNA through covalent and H bond interactions in the major groove. Molecular dynamic studies, RMSD and RMSF value analysis suggested the stable formation of complex between DNA and esculin. MMGBSA analysis revealed an energetically favourable interaction between esculin and DNA. Thus, esculin, a coumarin glycoside, can be developed as therapeutic agent, where a target biomolecule will be considered as DNA. Design of esculin based derivatives can be considered to develop DNA interactinganticancer agents.

Acknowledgement

Corresponding author is thankful to the Dean, Associate Dean of Department of Pharmaceutical sciences, School of Health Sciences and Technology of Dr. Vishwanath Karad MIT World Peace University, Kothrud, Pune.

Conflicts of interest

All authors declare no conflicts of interest.

References

1 Wang Y, Zhao M & Ye H, Comparative pharmacokinetic study of the main components of cortex fraxini after oral administration in normal and hyperuricemic rats. *Biomed Chromatogr*, 31 (2017) e3934.

2 Li ZY, Li XK & Lin Y, A comparative study of three chemometrics methods combined with excitation-emission matrix fluorescence for quantification of the bioactive compounds aesculin and aesculetin in *Cortex Fraxini*. *Front Chem*, 10 (2022) 984010.

3 Flores-Morales V, Villasana-Ruiz AP & Garza-Veloz I, Therapeutic effects of coumarins with different substitution patterns. *Molecules,* 28 (2023) 2413.

4 Rostom B, Karaky R & Kassab I, Coumarins derivatives and inflammation: review of their effects on the inflammatory signaling pathways. *Eur J Pharmacol*, 922 (2022) 174867.

5 Sinha S, Singh K & Ved A, Therapeutic journey and recent advances in the synthesis of coumarin derivatives. *Mini Rev Med Chem*,22 (2022) 1314.

6 Feng D, Zhang A & Yang Y, Coumarin-containing hybrids and their antibacterial activities. *Arch Pharm*, 353 (2020) e1900380.

7 Wu Y, Xu J & Liu Y, A review on anti-tumor mechanisms of coumarins. *Front Oncol*, 10 (2020) 592853.

8 Cai T, Cai & B, Pharmacological activities of esculin and esculetin: A review. *Medicine*, 102 (2023) E35306.

9 Erkkila KE, Odom DT, Barton J K, Recognition and reaction of metallointercalators with DNA. *Chem Rev*, 99 (1999) 2777.

10 Sousa SF, Fernandes PA & Ramos MJ, Protein-ligand docking: Current status and future challenges.*Struct. Fun Bioinfo*, 65 (2006) 15.

11 Trott O & Olson AJ, AutoDock Vina: improving the speed and accuracy of docking with a new scoring functionefficient optimization and multithreading. *J Comp Chem,* 31 (2010) 455.

12 Sanner MF, Python: a programming language for software integration and development. *J Mol Graph Model,* 17 (1999) 57.

13 Scior T, Mack HG, Guevara-Garcia JA & Koch W, Antidiabetic bis-Maltolato-Oxovanadium(IV): Conversion of inactive trans- to bioactive cis-BMOV for possible binding to target PTP-1B. *Drug Des Develop Therapy,* 2 (2008) 221.

14 Bowers KJ, Chow DE, Xu H, Dror RO, Eastwood MP, Gregersen BA, Klepeis JL, Kolossvary I, Moraes MA, Sacerdoti FD & Salmon JK, Scalable algorithms for molecular dynamics simulations on commodity clusters. InSC'06: Proceedings of the 2006 ACM/IEEE Conference on Supercomputing, 2006 43.

15 Chow E, Rendleman CA, Bowers KJ, Dror RO, Hughes DH, Gullingsrud J, Sacerdoti FD & Shaw DE, Desmond performance on a cluster of multicore processors. DE Shaw Research Technical Report, 2008.

16 Shivakumar D, Williams J, Wu Y, Damm W, Shelley J & Sherman W, Prediction of Absolute Solvation Free Energies using Molecular Dynamics Free Energy Perturbation and the OPLS Force Field. *J Chem Theory Comp*, 6(2010) 1509.

17 JorgensenWL, Chandrasekhar J, Madura J D, Impey R W & Klein ML, Comparison of simple potential functions for simulating liquid water. *J Chem Phys*, 79 (1983) 926.

18 Martyna GJ, Tobias DJ & Klein ML, Constant pressure molecular dynamics algorithms. *J Chem Phys*, 101 (1994) 4177.

19 Martyna GJ, Klein ML & Tuckerman M, Nose-Hoover chains-the canonical ensemble via continuous dynamics. *J Chem Phys*, 97 (1992) 2635.

20 ToukmajiA Y & Board J, Ewald summation techniques in perspective: a survey. *Comput Phys Commun,* 95 (1996) 73.

21 Saito ST, Silva G, Pungartnik C & Brendel M, Study of DNA–emodin interaction by FTIR and UV–vis spectroscopy. *J Photochem Photobiol B,* 111 (2012) 59.

22 Bai GY, Dong B, Lu YY, Wang KZ, Jin LP & Gao LH, A comparative study of the interaction of two structurally analogue ruthenium(II) complexes with DNA. *J Inorg. Biochem*, 98 (2004) 2011.

23 Wang XL, Chao H, Li H, Hong XL, Liu YJ, Tan LF & Ji LN, DNA interactions of cobalt(III) mixed-polypyridyl complexes containing asymmetric ligands. *J Inorg. Biochem,* 98 (2004) 1143.

24 Barton JK, Danishefsky AT & Goldberg JM, Tris (phenanthroline) ruthenium(II): stereoselectivity in binding to DNA. *J Am Chem Soc*, 106 (1984) 2172.

25 Chan HL, Liu QL, Tzeng BC, You YS, Peng SM, Yang M & Che CM, Syntheses of ruthenium(II) quinonediimine complexes of cyclam and characterization of their DNA-binding activities and cytotoxicity. *Inorg. Chem*, 41 (2002) 3161.

26 Nguyen B, Neidle S & Wilson WD, A role of water molecules in DNA –ligand minor groove recognition. *Acc Chem Res*, 42 (2009) 11.

27 Sharma P, Gopi P, Singh S, Sudha Rani MS & Pandya P, Binding studies of sertraline hydrochloride with CT-DNA using experimental and computational techniques. *Spectrochimica Acta Part A: Molecular and Biomolecular Spectroscopy*, 300 (2023) 122910.

28 Pavithra K, Durga Priyadarshini R, Vennila KN & Elango KP, Multi-spectroscopic and molecular simulation methods of analysis to explore the mode of binding of Mebendazole drug with calf-thymus DNA. *Spectrochim Acta A Mol Biomol Spectrosc*, 300 (2023) 122938.

29 Wang D, Liu M, Wu Y, Weng T, Wang L, Zhang Y, Zhao Y & Han J, Idarubicin/mithramycin-acridine orange combination drugs co-loaded by DNA nanostructures: Different effects of intercalation and groove binding on drug release and cytotoxicity. *J Mol Liquids*, 355 (2022) 118947.

30 Quraishi S, Saha D, Kumari K, Jha AN & Roy AS, Non-covalent binding interaction of bioactive coumarin aesculetin with calf thymus DNA and yeast transfer RNA: A detailed investigation to decipher the binding affinities, binding location, interacting forces and structural alterations at a molecular level. *Int J Biol Macro,* 257 (2024) 128568.

31 Amir HM, Mubarak IH, Sarwar T & Rehmaan SU, Interaction of indomethacin with calf thymus DNA: A multi-spectroscopic, thermodynamic and molecular modelling approach. *Medchemcomm,* 8 (2022) 1283.

32 Ivanov VI, Minchenkova LE, Chyolkina, AE & Poletayev AI, Different conformations of double-stranded nucleic acid in solution as revealed by circular dichroism. *Biopolymers*, 12 (1973) 89.

33 Meenongwa A, Brissos RF, Soikum C, Chaveerach P, Gamez Y & Trongpanich U, DNA-interacting and biological properties of copper(II) complexes from amidino-O-methylurea. *New J Chem*, 39 (2015) 664.

34 Bai GY, Dong B, Lu Y, Wang KZ, Jin LP & Gao LH, A comparative study of the interaction of two structurally analogue ruthenium(II) complexes with DNA. *J Inorg Biochem*, 98 (2004) 2011.

35 Senthil Raja D, Bhuvanesh NP & Natarajan K, Structure activity relationship study of copper(II) complexes with 2-oxo-1,2-dihydroquinoline-3-carbaldehyde(4-methylbenzoyl) hydrazone: synthesis, structures, DNA and protein interaction studies, antioxidative and cytotoxic activity. *J Biol Inorg Chem*, 17 (2012) 223.

36 Pavithra K, Priyadharshini DR, Vennila KN & Elango KP, Exploring the binding mechanism of Pomalidomide drug with CT-DNA: Insights from multi-spectroscopic, molecular docking and simulation studies. *J Mol Struct*, 1302 (2024) 137547.

37 Sarwar T, Husain MA, Rehman SU, Ishqi HM & Tabish M, Multi-spectroscopic and molecular modelling studies on the interaction of esculetin with calf thymus DNA. *Mol Biosystem*, 11 (2015) 522.